Inhibition of Carcinoma Cell Motility by Epoxyeicosatrienoic Acid (EET) Antagonists

Kasem Nithipatikom[1], **Daniel M. Brody**[1], **Alan T. Tang**[1], **Vijaya L. Manthati**[2], **John R. Falck**[2], **Carol L. Williams**[1], and **William B. Campbell**[1]

[1]Department of Pharmacology and Toxicology, Medical College of Wisconsin, 8701 Watertown Plank Road, Milwaukee, WI 53226

[2]Departments of Biochemistry and Pharmacology, University of Texas Southwestern Medical Center, Dallas, TX 75390

Summary

Cytochrome P450 (CYP) epoxygenases, CYP2C8, 2C9 and 2J2 mRNAs and proteins, were expressed in prostate carcinoma (PC-3, DU-145 and LNCaP) cells. 11,12-Epoxyeicosatrienoic acid (11,12-EET) was the major arachidonic acid metabolite in these cells. Blocking the EET synthesis by a selective CYP epoxygenase inhibitor (MS-PPOH) inhibited tonic (basal) invasion and migration (motility) while exogenously added EETs induced cell motility in a concentration-dependent manner. An EGFR kinase inhibitor (AG494) or a PI3 kinase inhibitor (LY294002) inhibited cell migration and reduced 11,12-EET-induced cell migration. Importantly, synthetic EET antagonists (14,15-EEZE, 14,15-EEZE-PEG and 14,15-EEZE-mSI) inhibited EET-induced cell invasion and migration. 11,12-EET induced cell stretching and myosin-actin microfilament formation as well as increased phosphorylation of EGFR and Akt (Ser473) while 14,15-EEZE inhibited these effects. These results suggest that EETs induce and EET antagonists inhibit cell motility, possibly by putative EET receptor-mediated EGFR and PI3K/Akt pathways, and suggest EET antagonists as potential therapeutic agents for prostate cancer.

Keywords

Cytochrome P450 epoxygenases; EETs; EET antagonists; cell motility; prostate cancer

Introduction

CYP epoxygenases metabolize arachidonic acid (AA) to 5,6-, 8,9-, 11,12-, and 14,15-epoxyeicosatrienoic acid (EET). In humans, multiple CYPs including CYP2C8, 2C9, and 2J2 convert AA to EETs.[1,2] Their catalytic efficiency and regio-selectivity of EET synthesis are isoform- and species-specific.[3,4] EETs stimulate proliferation, angiogenesis, and migration of endothelial cells.[5,6] Our previous studies in cardiovascular systems suggest that EETs bind to a putative binding protein or receptor(s) to initiate signaling,[7,8] although the protein(s) has not been fully characterized. Thus, this uncharacterized binding protein will be referred as "a putative receptor". Numerous synthetic compounds have been developed as EET antagonists and used to antagonize the actions of the EETs in vascular systems.[9,10]

Corresponding author: Kasem Nithipatikom, Ph.D., Department of Pharmacology and Toxicology, Medical College of Wisconsin, 8701 Watertown Plank Road, Milwaukee, Wisconsin 53226, (414) 456-8605, (414) 456-6545 Fax, kasemn@mcw.edu.

Numerous CYP epoxygenase mRNAs including CYP2C8, 2J2 and 2C9 are differentially expressed in the human prostate gland[4,11] and proteins of the CYP2C family are present in malignant prostate tissue samples,[12,13] suggesting potential roles of CYP epoxygenases and EETs in prostate cancer. Since EETs stimulate cell migration of several cell types,[5,14,15] we determined the roles of EETs in the regulation of motility of prostate carcinoma cells and possible signaling pathways of the EETs in this regulation. Furthermore, we determined whether a group of synthetic compounds, known for their ability to antagonize the actions of the EETs in vascular systems,[9,10] can block the EET-induced cell motility. These EET antagonists may represent new potential therapeutic agents in treatment of prostate cancer.

Materials and Methods

Materials

PC-3, DU-145 and LNCaP cells were obtained from the American Type Culture Collection (Rockville, MD). Eagle's minimal essential medium (RPMI) was obtained from Invitrogen (Carlsbad, CA). AA, EGF, miconazole, and LY294002 were obtained from Sigma Chemical (St. Louis, MO). AG-494, 14,15-EET, 11,12-EET, 8,9-EET, 5,6-EET, $[^2H_8]$14,15-EET, and 17-ODYA were obtained from Cayman Chemical (Ann Arbor, MI). 14,15-EEZE, 14,15-EEZE-PEG, 14,15-EEZE-mSI, and MS-PPOH were synthesized in Dr. Falck's laboratory. RT^2 Real-Time SYBR Green/Fluorescein PCR Master Mix and primers for CYP2C8, CYP2C9, CYP2J2, and HPRT1 were obtained from SuperArray (Frederick, MD). Primary antibody against CYP2C8/9/19 was from Millipore (Billerica, MA), CYP2C9 was from Abcam Inc. (Cambridge, MA) and MorphoSys US Inc. (Raleigh, NC), and CYP2C8 was generously provided by Dr. Capdevila (Vanderbilt University, TN). Primary antibodies against Akt, phospho-Akt (Ser473), and EGFR were obtained from Cell Signaling Technologies (Danvers, MA). Bio-Plex Phospho-EGFR (Tyr) Assay Kit was obtained from BioRad (Hercules, CA). Goat anti-rabbit IgG-HRP was obtained from Zymed Laboratories (South San Francisco, CA). SA-2 human IgM antibody and FITC-labeled anti-human IgM were provided by Dr. Williams.[16] Transwell® plates with filters (8-um pore) were obtained from Corning Inc. (Corning, NY). Matrigel was obtained from BD Biosciences (Bedford, MA). ECL Western blot detection kit and BCA protein assay kit were obtained from Pierce (Rockville, IL). Distilled and deionized water was used in all experiments.

Cell culture

PC-3, DU-145 and LNCaP cells were cultured in RPMI containing fetal bovine serum (10%), L-glutamine (1%), and penicillin/streptomycin (1%) at 37°C in 5% CO_2. Cells were grown to approximately 60-70% confluency prior to all experiments except for the migration assay.

Quantitative reverse-transcriptase polymerase chain reaction of CYP epoxygenases and HPRT1

Total RNAs were extracted from cells using Trizol reagent (Invitrogen) followed by treatment with RNase-free DNAase I. One microgram was reverse-transcribed using oligo-dT primers with SuperScript III First-Strand Synthesis Kit (Invitrogen). Sample mRNAs were quantified using RT^2 Real-Time SYBR Green/Fluorescein PCR Master Mix with human CYP2C8, CYP2C9, CYP2J2, and HPRT1 primers (SuperArray). PCR cycling conditions were: 95°C for 10 min, 45 cycles at 95°C for 30 sec, 55°C for 60 sec, and finally at 72°C for 30 sec (BioRad iCycler). The relative expression of CYP epoxygenases was normalized to HPRT1 for each cell line and compared to CYP2C9 of PC-3 cells (the lowest expression among the prostate carcinoma cells).

Measurement of EETs

Samples were added with $[^2H_8]14,15$-EET as an internal standard, isolated by solid phase extraction, and EETs were analyzed by using LC-ESI-MS (Agilent 1100 LC-MSD, SL model) as previously described.[17] For quantitative measurement, m/z 319 and 327 were used for four regioisomeric EETs and $[^2H_8]14,15$-EET (internal standard), respectively. Then, EET concentrations were normalized to protein content using the BCA protein assay.

Immunofluorescence imaging of microfilaments

To examine actin-myosin organization, cells were cultured on coverslips in 12-well plates in complete medium for 48 h. Cells were treated with vehicle or 11,12-EET, 14,15-EEZE, or a combination of 11,12-EET and 14,15-EEZE for 90 min. Then, cells were fixed and incubated with the SA-2 human IgM antibody to the myosin heavy chain and FITC-labeled anti-human IgM as previously described.[16] The cell images were captured using a Nikon Eclipse E600 fluorescence microscope.

Cell invasion assay

Cell invasion was determined using Boyden Chambers with Transwell inserts containing filters coated with Matrigel as previously described.[18,19] Pharmacological agents such as 14,15-EET, 11,12-EET, EET antagonists (14,15-EEZE, 14,15-EEZE-PEG and 14,15-EEZE-mSI), MS-PPOH, miconazole, 17-ODYA, or combinations of these agents were added to the cells during the assay. Human fibroblast (ATCC) conditioned-media (400 μL) was added in the bottom compartment of the well as a chemoattractant. An additional 6 wells per treatment without Matrigel or Transwells but containing the identical number of cells and pharmacological agents were used for the "control counts" of the thymidine [methyl-^{3}H] (Perkin Elmer) to assess any changes or difference in cell numbers between control cells and pharmacologically treated cells due to cell proliferation or cell death. Cells were incubated at 37°C in the incubator for 5 h. Each treatment was repeated 2-3 times. The invasion was reported as the percentage of the invasion of the control cells.

Cell migration assay

Cell migration was determined by *in vitro* wound healing assay as previously described.[16] Cells were treated with 14,15-EET, 11,12-EET, 14,15-EEZE, 14,15-EEZE-PEG, 14,15-EEZE-mSI, MS-PPOH, miconazole, LY294002, AG-494, or combinations of these pharmacological agents in serum-free media. Photographs of the wounds were taken at 0-h and after 24-h incubation at 37°C. Each treatment was performed in 3 dishes and repeated in two or three separate experiments. Migration was determined by the difference (in μm) between the initial wound widths (0 h) and the final wound widths (24 h) and normalized to the percentage of migration of the control cells.

Cell viability

Cells were treated with the same conditions used in the invasion and migration assays and then cell viability and proliferation were determined using the trypan blue assay (Sigma Chemical)[20] and/or the MTT assay (Sigma Chemical)[21] to assure that the observed changes in cell migration were not from cell proliferation or cell death.

Western blot analysis

Proteins were separated on SDS-PAGE BioRad Ready Gels (10%). Protein loading and β-actin were used as loading controls. Blots were incubated with primary antibodies against CYP2C8/9/19, CYP2C8, CYP2C9, p-Akt (Ser473) (1:1000), total-Akt (1:1000), or total-EGFR (1:1000) followed by goat anti-rabbit IgG-HRP (1:3000). Total EGFR (t-EGFR) expression was used for comparison of the p-EGFR results obtained from the Bio-Plex assay

(see below). Detection was made by using ECL Western Blotting Substrate (Pierce) and captured by Fuji film X-ray (Tokyo, Japan). Band densities were analyzed using Image J software from the NIH.

Determination of phospho-EGFR using Bio-Plex phosphoprotein assay

PC-3 cells were treated with 11,12-EET or 14,15 EEZE for 1, 5, 15, 30, 60, and 120 min and lysed as above. Then, p-EGFR (Tyr) was determined using Bio-Plex Phospho-EGFR (Tyr) Assay Kit following the provided protocol. EGF (0.5 ng/mL) treatment was used as an experimental positive control and the kit-supplied samples of untreated HeLa cells were used as a negative control. Briefly, in a 96-well filter plate, bead solution and sample were added and incubated at room temperature, washed, the antibody for p-EGFR was added and incubated at room temperature and washed. Then, Streptavidin-PE working dilution was added, incubated, washed, and Bio-Plex Bead resuspension buffer was added. The plate was shaken for 30 sec and the samples were measured on the Bio-Plex reader. Relative fluorescence signal in each well corresponds to the relative level of p-EGFR (Tyr).

Statistical analysis

The means of the measured values of each treatment group were compared using Student's t-test (two tailed). Means were considered statistically different from one another if $P < 0.05$.

Results

Expression of CYP epoxygenases

The relative CYP2C8, CYP2C9, and CYP2J2 mRNAs in PC-3, DU-145, and LNCaP cells was compared with the reference HPRT1 gene.[22] Then, they were normalized to mRNA of CYP2C9 in PC-3 cells (a relative expression of 1.00). *CYP* mRNAs varied among cell lines. The relative expression of CYP2C8 mRNA in prostate carcinoma cells was in the order of DU-145 > PC-3 ≈ LNCaP cells, CYP2C9 mRNA was in the order of LNCaP > DU-145 ≈ PC-3 cells, and CYP2J2 mRNA was in the order of LNCaP ≈ DU-145 > PC-3 cells (Fig. 1A).

CYP2C8/9/19, CYP2C8 and CYP2C9 proteins were determined by Western blot analysis. Interestingly, the most intense immunoreactive band of CYP2C8/9/19 was observed in LNCaP cells and decreased in PC-3 > DU-145 cells. Immunoreactive bands of CYP2C8 and 2C9 were also relatively higher in LNCaP cells than in PC-3 and DU-145 cells (Fig. 1B). Relative intensity of immunoreactive bands of CYP2C8/9/19, 2C8 and 2C9 to β-actin in these prostate carcinoma cells was summarized (Fig. 1C). Again, the expression of proteins was normalized to the expression of that CYP epoxygenase in PC-3 cells (a relative expression of 1.00). Primary antibody against CYP2J2 was not available for this study.

Regioisomers and concentrations of EETs

In prostate carcinoma cells, 11,12-EET was the major metabolite (Fig. 1D) and 14,15-EET was the second most abundant isomer (Fig. 1E), while 8,9-EET and 5,6-EET were produced at very low or undetectable concentrations. Among prostate carcinoma cell lines, PC-3 cells produced 11,12-EET at higher concentrations than in DU-145 and LNCaP cells. DU-145 cells produced the lowest concentrations of 14,15-EET.

Since EETs can be hydrolyzed by soluble epoxide hydrolase (sEH) to their corresponding regioisomers of dihydroxyeicosatrienoic acids (DHETs), the concentrations of DHETs were determined by LC-ESI-MS[17] to evaluate whether the hydrolysis of EETs may contribute to the effects of EETs on cell motility. Concentrations of 11,12-DHET (hydrolytic product of 11,12-EET) were 12.33±2.55, 5.33±3.11, and 11.67±1.86 pg/mg protein for PC-3, DU-145,

and LNCaP cells, respectively, indicating that the hydrolysis of EETs to DHETs in these cells was low. Furthermore, exogenously added 11,12-DHET (0.1, 1.0 and 10.0 µmol/L) did not significantly change cell invasion or migration (data not shown).

Effects of EETs and inhibitors of EET synthesis on cell motility

Prostate carcinoma cells were treated with 11,12-EET or 14,15-EET at different concentrations during the invasion or migration assay. 11,12-EET increased invasion and migration of PC-3 cells in a concentration-dependent manner (Fig. 2A). Identical results were obtained with 14,15-EET treatment and also in DU-145 and LNCaP cells (data not shown).

Blocking cellular EET synthesis by a selective CYP epoxygenase inhibitor, MS-PPOH, inhibited tonic (basal) cell invasion and migration and reduced the 11,12-EET-induced cell motility (Fig. 2B). In a separate experiment, PC-3 cells were treated with MS-PPOH (10.0 µmol/L) at 37°C for 30 min, cells were lyzed and EETs were determined by LC-ESI-MS[17] Concentrations of 11,12-EET and 14,15-EET were significantly lower in MS-PPOH-treated PC-3 cells than control cells (Fig. 2C). Similar decreases of cell motility were observed with CYP inhibitors, miconazole and 17-ODYA. (Invasion was reduced to $72.0 \pm 8.8\%$ and $22.6 \pm 7.5\%$ for miconazole at 10.0 and 50.0 µmol/L, respectively and $53.5 \pm 6.4\%$ for 17-ODYA at 10.0 µmol/L; migration was reduced to $47.5 \pm 2.8\%$ for miconazole at 30.0 µmol/L and $79.9 \pm 7.0\%$ for a combination of miconazole at 30.0 µmol/L and 11,12-EET at 1.0 µmol/L). These results indicate that endogenously produced EETs mediate a tonic motility of prostate carcinoma cells and the blockade of EET synthesis reduces the tonic motility.

Effects of the inhibition of EGFR kinase and phosphatidylinositol 3-kinase (PI3K) on cell motility

To determine the effects of inhibition of EGFR kinase on cell migration, PC-3 cells were treated with an EGFR kinase inhibitor, AG-494 during the migration assay. AG494 inhibited cell migration and it also reduced the EET-induced cell migration (Fig. 3A). These results suggest that EET stimulates cell migration, possibly through the trans-activation of EGFR.

To determine the effect of inhibition of phosphatidylinositol 3-kinase (PI3K) on cell migration, PC-3 cells were treated with a PI3K inhibitor, LY294002 during the migration assay. LY294002 inhibited cell migration and it also reduced the 11,12-EET-induced migration of PC-3 cells (Fig. 3B). These results suggest that the actions of the EETs on cell motility may involve the activation of PI3K/Akt pathway.

Cell morphology and myosin microfilament organization

To determine the changes in cell shapes and organization of actin/myosin microfilaments, PC-3 cells were treated with 11,12-EET, 14,15-EEZE, or a combination of 11,12-EET and 14,15-EEZE for 90 min. Then, the cells were fixed and stained for myosin heavy chain[16] (Fig. 4A). Myosin-containing stress fibers were present in control PC-3 cells (Fig. 4A, panel a), indicating an association between myosin and actin. 11,12-EET induced the cells to stretch out and exhibit more apparent myosin microfilaments (Fig. 4A, panel b), indicating an increased myosin-actin association. However, 14,15-EEZE diminished myosin-containing stress fibers (Fig. 4A, panel c), indicating a lack of myosin-actin association. 14,15-EEZE also induced significant changes of the cell shape to become rounded and smaller. Furthermore, 14,15-EEZE reduced the effects of 11,12-EET-induced cell stretching and myosin-actin association (Fig. 4A, panel d). Cells were viable under these treatments.

Effects of putative EET receptor antagonists on cell invasion and migration

To determine the effects of synthetic EET antagonists on cell invasion and migration, PC-3 cells were treated with 14,15-EEZE, 14,15-EEZE-PEG, 14,15-EEZE-mSI, 11,12-EET, and combinations of these EET antagonists and 11,12-EET during the invasion assay and migration assays. 11,12-EET stimulated but 14,15-EEZE blocked the migration of PC-3 cells (Fig. 4B). EET antagonists alone inhibited the tonic invasion and migration and blocked the 11,12-EET-induced cell invasion/migration of PC-3 cells (Fig. 4C and 4D). The effects of 11,12-EET and 14,15-EEZE on migration in DU-145 and LNCaP cells were similar to PC-3 cells (data not shown). These results further indicate that EETs stimulate cell motility possibly through the interaction of EETs with a putative binding protein/receptor(s) and the activity is blocked by the synthetic EET receptor antagonists.

Effects of 11,12-EET and EET antagonist on the activation of EGFR

The activation of EGFR by 11,12-EET and 14,15-EEZE in PC-3 cells was determined by measuring p-EGFR (Tyr) using Bio-Plex assay. 11,12-EET activated EGFR in a time-dependent manner as indicated by the fluorescence signal that represents the level of p-EGFR (Tyr). Total EGFR for each time point was determined by Western blot analysis and used for normalizing p-EGFR (Fig. 5A). Vehicle-treated cells were examined at two time points of 1 min and 120 min. The EET treatment of cells increased p-EGFR with time with a maximal activation at 5 min and the activated EGFR decreased to the control level after 60 min.

PC-3 cells were treated with 11,12-EET, 14,15-EEZE, and a combination of 11,12-EET and 14,15-EEZE for 5 min, and p-EGFR was determined by Bio-Plex assay. Again, 11,12-EET increased p-EGFR but 14,15-EEZE decreased p-EGFR and it also blocked the activation of EGFR by 11,12-EET (Fig. 5B).

Effects of 11,12-EET and EET antagonist on the activation of PI3K/Akt

PC-3 cells were treated with 11,12-EET at various times and p-Akt (p-Ser473) and t-Akt were determined by Western blot analysis. The immunoreactive band ratio of p-Akt to t-Akt indicated that 11,12-EET activated Akt as a function of time with the maximal activation about 30-60 min (Fig. 5C). 11,12-EET also activated Akt in LNCaP cells with the maximal activation about 60 min similar to PC-3 cells (data not shown). PC-3 cells were treated with 11,12-EET, 14,15-EEZE, and a combination of 14,15-EEZE and 11,12-EET for 60 min and p-Akt (p-Ser473) measured by Western blot analysis. 11,12-EET activated Akt but 14,15-EEZE inhibited the phosphorylation of Akt and it also blocked the EET-activated Akt (Fig. 5D).

Discussion

Prostate carcinoma (PC-3, DU-145 and LNCaP) cells have differential expression of CYP mRNAs and proteins. Interestingly, the mRNA expression, protein expression and EET concentrations in these cells did not appear to have obvious correlations. For example, LNCaP cells had the highest mRNAs of CYP2C9 and 2J2 and the highest immunoreactive bands for CYP2C8, 2C9 and 2C8/9/19 among prostate carcinoma cells. However, PC-3 cells, but not LNCaP cells, had the highest endogenous 11,12-EET concentrations (Fig. 1C). These results suggest that PC-3 cells may have higher epoxygenase activity or may express other CYP epoxygenases. Since CYP2J2 mRNA was detected, it is possible that these carcinoma cells express CYP2J2 protein; although a previous study did not detect CYP2J2 in prostate adenocarcinoma tissues.[13] In addition to these three well-characterized CYP epoxygenases, the synthesis of EETs by other CYP epoxygenases[1,23] in prostate carcinoma cells cannot be ruled out.

Although EETs stimulate migration and invasion of various cell types[14] including some carcinoma cell lines,[15] the mechanisms underlying these effects are not fully understood. EETs induced-changes in actin-myosin microfilaments suggest that EETs may stimulate a variety of signaling pathways including the activation of EGFR and PI3/Akt pathways.[24,25] The activation of EGFR by the cross-talk with other ligand-activated G-protein-coupled receptors has been documented.[26] Previous studies of EETs and EET antagonists suggested that EETs may bind to putative binding protein or receptor(s)[7,8] which may trans-activate EGFR and Akt in the regulation of cell motility.[6,27,28] A protein tyrosine kinase (PTK) inhibitor, AG-494 inhibited cell migration and reduced the EET-activated cell migration similar to other PTK inhibitors, genistein and tyrphostin AG-1478.[29] A PI3K inhibitor, LY294002 also inhibited prostate carcinoma cell migration and reduced the EET-activated cell migration. These results suggest that EETs possibly transactivate EGFR and subsequent PI3K/Akt pathways to stimulate motility of prostate carcinoma cells.

11,12-EET induced PC-3 cells to stretch out and form more apparent actin-myosin microfilaments. Conversely, 14,15-EEZE diminished myosin-containing microfilaments, indicating that the cells had decreased myosin-actin association. Furthermore, 14,15-EEZE induced significant morphologic changes that caused the cells to become more rounded and smaller. The cytoskeletal changes suggest that 11,12-EET may induce cell motility while EET antagonists such as 14,15-EEZE may block cell motility and reduce the effects of EETs.

Importantly, synthetic EET antagonists, 14,15-EEZE, 14,15-EEZE-PEG and 14,15-EEZE-mSI diminished the tonic invasion/migration and reduced 11,12-EET-induced cell motility. These results indicate that EETs are endogenous stimulators of prostate carcinoma cell motility and EET antagonists inhibit the actions of endogenous EETs, suggesting the activation/deactivation of putative EET binding protein or receptor(s).[7,8] EET antagonists reduced the EETs-activated phosphorylation of EGFR and Akt. Taken together, these results indicate that EET antagonists inhibit motility of prostate carcinoma cells, possibly through the antagonism of the putative EET receptor-mediated EGFR activation and subsequent PI3K/Akt pathways as summarized in the proposed diagram (Fig. 6). These synthetic EET antagonists exhibit therapeutic potential for prostate cancer.

Acknowledgments

References

1. Rifkind AB, Lee C, Chang TK, et al. Arachidonic acid metabolism by human cytochrome P450s 2C8, 2C9, 2E1, and 1A2: regioselective oxygenation and evidence for a role for CYP2C enzymes in arachidonic acid epoxygenation in human liver microsomes. Arch Biochem Biophys. 1995; 320:380–9. [PubMed: 7625847]

2. Lundblad MS, Stark K, Eliasson E, et al. Biosynthesis of epoxyeicosatrienoic acids varies between polymorphic CYP2C enzymes. Biochem Biophys Res Commun. 2005; 327:1052–7. [PubMed: 15652503]

3. Imaoka S, Hashizume T, Funae Y. Localization of rat cytochrome P450 in various tissues and comparison of arachidonic acid metabolism by rat P450 with that by human P450 orthologs. Drug Metab Pharmacokinet. 2005; 20:478–84. [PubMed: 16415532]

4. Nishimura M, Yaguti H, Yoshitsugu H, et al. Tissue distribution of mRNA expression of human cytochrome P450 isoforms assessed by high-sensitivity real-time reverse transcription PCR. Yakugaku Zasshi. 2003; 123:369–75. [PubMed: 12772594]

5. Michaelis UR, Fissthaler B, Barbosa-Sicard E, et al. Cytochrome P450 epoxygenases 2C8 and 2C9 are implicated in hypoxia-induced endothelial cell migration and angiogenesis. J Cell Sci. 2005; 118:5489–98. [PubMed: 16291720]

6. Wang Y, Wei X, Xiao X, et al. Arachidonic acid epoxygenase metabolites stimulate endothelial cell growth and angiogenesis via mitogen-activated protein kinase and phosphatidylinositol 3-kinase/ Akt signaling pathways. J Pharmacol Exp Ther. 2005; 314:522–32. [PubMed: 15840765]

7. Yang W, Tuniki VR, Anjaiah S, et al. Characterization of epoxyeicosatrienoic acid binding site in U937 membranes using a novel radiolabeled agonist, 20-125i-14,15-epoxyeicosa-8(Z)-enoic acid. J Pharmacol Exp Ther. 2008; 324:1019–27. [PubMed: 18171909]

8. Yang W, Holmes BB, Gopal VR, et al. Characterization of 14,15-epoxyeicosatrienoyl-sulfonamides as 14,15-epoxyeicosatrienoic acid agonists: use for studies of metabolism and ligand binding. J Pharmacol Exp Ther. 2007; 321:1023–31. [PubMed: 17327488]

9. Gauthier KM, Jagadeesh SG, Falck JR, et al. 14,15-epoxyeicosa-5(Z)-enoic-mSI: a 14,15- and 5,6-EET antagonist in bovine coronary arteries. Hypertension. 2003; 42:555–61. [PubMed: 12953017]

10. Gauthier KM, Deeter C, Krishna UM, et al. 14,15-Epoxyeicosa-5(Z)-enoic acid: a selective epoxyeicosatrienoic acid antagonist that inhibits endothelium-dependent hyperpolarization and relaxation in coronary arteries. Circ Res. 2002; 90:1028–36. [PubMed: 12016270]

11. Ragavan N, Hewitt R, Cooper LJ, et al. CYP1B1 expression in prostate is higher in the peripheral than in the transition zone. Cancer Lett. 2004; 215:69–78. [PubMed: 15374634]

12. Yokose T, Doy M, Taniguchi T, et al. Immunohistochemical study of cytochrome P450 2C and 3A in human non-neoplastic and neoplastic tissues. Virchows Arch. 1999; 434:401–11. [PubMed: 10389623]

13. Enayetallah AE, French RA, Grant DF. Distribution of soluble epoxide hydrolase, cytochrome P450 2C8, 2C9 and 2J2 in human malignant neoplasms. J Mol Histol. 2006; 37:133–41. [PubMed: 16957870]

14. Michaelis UR, Xia N, Barbosa-Sicard E, et al. Role of cytochrome P450 2C epoxygenases in hypoxia-induced cell migration and angiogenesis in retinal endothelial cells. Invest Ophthalmol Vis Sci. 2008; 49:1242–7. [PubMed: 18326754]

15. Jiang JG, Ning YG, Chen C, et al. Cytochrome p450 epoxygenase promotes human cancer metastasis. Cancer Res. 2007; 67:6665–74. [PubMed: 17638876]

16. Tew GW, Lorimer EL, Berg TJ, et al. SmgGDS Regulates Cell Proliferation, Migration, and NF-{kappa}B Transcriptional Activity in Non-small Cell Lung Carcinoma. J Biol Chem. 2008; 283:963–76. [PubMed: 17951244]

17. Nithipatikom K, Grall AJ, Holmes BB, et al. Liquid chromatographic-electrospray ionization-mass spectrometric analysis of cytochrome P450 metabolites of arachidonic acid. Anal Biochem. 2001; 298:327–36. [PubMed: 11700990]

18. Nithipatikom K, Endsley MP, Isbell MA, et al. 2-Arachidonoylglycerol: A novel inhibitor of androgen-independent prostate cancer cell invasion. Cancer Res. 2004; 64:8826–30. [PubMed: 15604240]

19. Endsley MP, Aggarwal N, Isbell MA, et al. Diverse roles of 2-arachidonoylglycerol in invasion of prostate carcinoma cells: Location, hydrolysis and 12-lipoxygenase metabolism. Int J Cancer. 2007; 121:984–91. [PubMed: 17443494]

20. Mimeault M, Pommery N, Wattez N, et al. Anti-proliferative and apoptotic effects of anandamide in human prostatic cancer cell lines: implication of epidermal growth factor receptor down-regulation and ceramide production. Prostate. 2003; 56:1–12. [PubMed: 12746841]

21. Yang P, Collin P, Madden T, et al. Inhibition of proliferation of PC3 cells by the branched-chain fatty acid, 12-methyltetradecanoic acid, is associated with inhibition of 5-lipoxygenase. Prostate. 2003; 55:281–91. [PubMed: 12712407]

22. Ohl F, Jung M, Xu C, et al. Gene expression studies in prostate cancer tissue: which reference gene should be selected for normalization? J Mol Med. 2005; 83:1014–24. [PubMed: 16211407]

23. Choudhary D, Jansson I, Stoilov I, et al. Metabolism of retinoids and arachidonic acid by human and mouse cytochrome P450 1b1. Drug Metab Dispos. 2004; 32:840–7. [PubMed: 15258110]

24. Zhou W, Grandis JR, Wells A. STAT3 is required but not sufficient for EGF receptor-mediated migration and invasion of human prostate carcinoma cell lines. Br J Cancer. 2006; 95:164–71. [PubMed: 16804520]

25. Marcoux N, Vuori K. EGF receptor activity is essential for adhesion-induced stress fiber formation and cofilin phosphorylation. Cell Signal. 2005; 17:1449–55. [PubMed: 16125057]

26. Schwartz MA, Baron V. Interactions between mitogenic stimuli, or, a thousand and one connections. Curr Opin Cell Biol. 1999; 11:197–202. [PubMed: 10209147]

27. Jiang JG, Chen CL, Card JW, et al. Cytochrome P450 2J2 promotes the neoplastic phenotype of carcinoma cells and is up-regulated in human tumors. Cancer Res. 2005; 65:4707–15. [PubMed: 15930289]

28. Zhang B, Cao H, Rao GN. Fibroblast growth factor-2 is a downstream mediator of phosphatidylinositol 3-kinase-Akt signaling in 14,15-epoxyeicosatrienoic acid-induced angiogenesis. J Biol Chem. 2006; 281:905–14. [PubMed: 16286479]

29. Skogseth H, Larsson E, Halgunset J. The invasive behaviour of prostatic cancer cells is suppressed by inhibitors of tyrosine kinase. Apmis. 2006; 114:61–6. [PubMed: 16499663]

30. Chen JK, Capdevila J, Harris RC. Heparin-binding EGF-like growth factor mediates the biological effects of P450 arachidonate epoxygenase metabolites in epithelial cells. Proc Natl Acad Sci U S A. 2002; 99:6029–34. [PubMed: 11983897]

31. Cheng LM, Jiang JG, Sun ZY, et al. The epoxyeicosatrienoic acid-stimulated phosphorylation of EGF-R involves the activation of metalloproteinases and the release of HB-EGF in cancer cells. Acta Pharmacol Sin. 2010; 31:211–8. [PubMed: 20139904]

32. Dhanasekaran A, Gruenloh SK, Buonaccorsi JN, et al. Multiple antiapoptotic targets of the PI3K/Akt survival pathway are activated by epoxyeicosatrienoic acids to protect cardiomyocytes from hypoxia/anoxia. Am J Physiol Heart Circ Physiol. 2008; 294:H724–35. [PubMed: 18055514]

Abbreviations

|	
AA	arachidonic acid
CYP epoxygenase	cytochrome P450 epoxygenase
DHET	dihydroxyeicosatrienoic acid
EET	epoxyeicosatrienoic acid
14,15-EEZE	14,15-epoxyeicosa-5(Z)-enoic acid
14,15-EEZE-PEG	14,15-epoxyeicosa-5(Z)-enoic acid 2-[2-(3-hydroxy-propoxy)-ethoxy]-ethyl ester
14,15-EEZE-mSI	14,15-epoxyeicosa-5(Z)-enoic-methylsulfonylimide
HPRT1	hypoxanthine phosphoribosyltransferase 1
MS-PPOH	N-methylsulfonyl-6-(2-propargyloxyphenyl)hexanamide
ODYA	17-octadecynoic acid
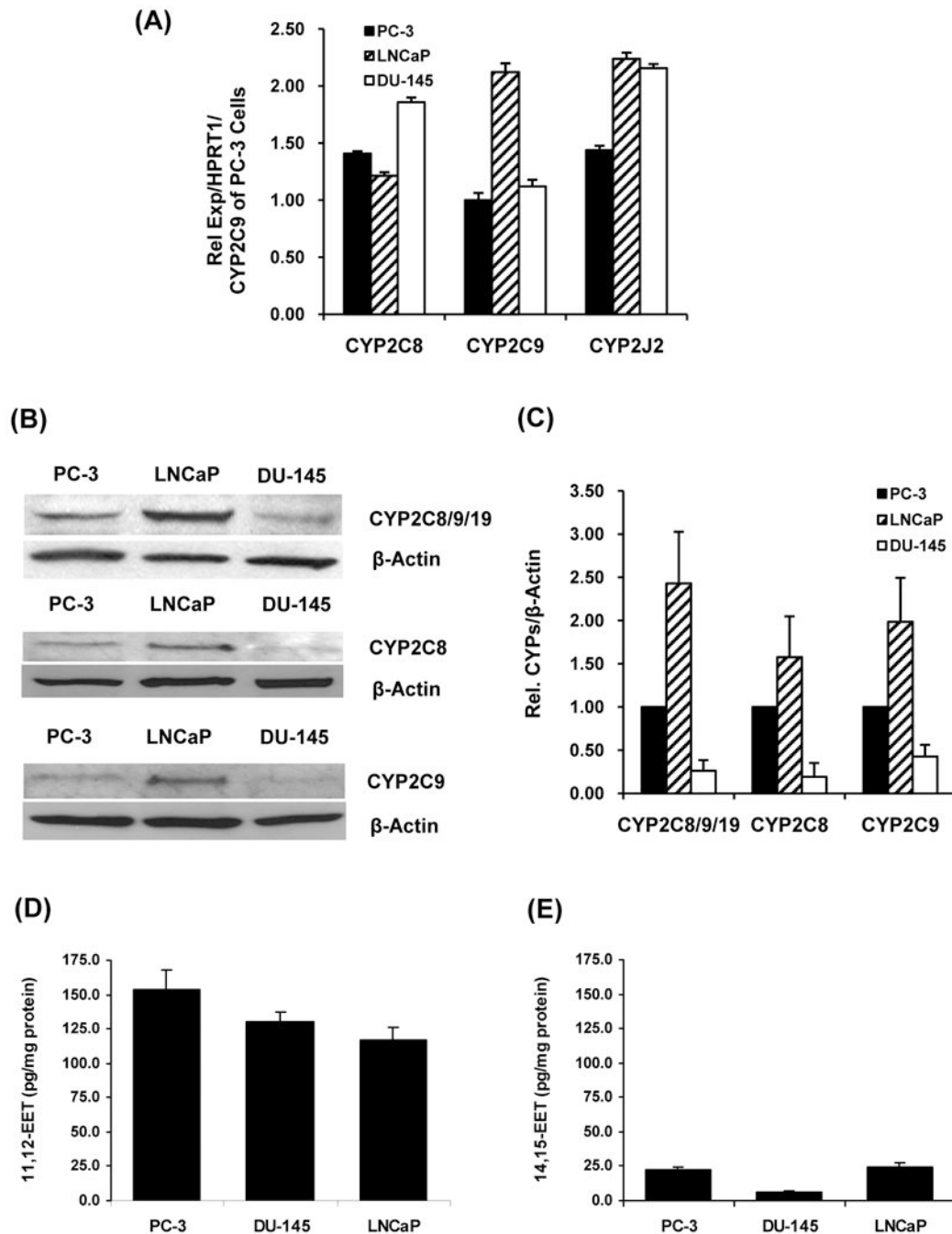
Figure 1.
Expression of CYP2C8, 2C9 and 2J2 and concentrations of EETs in human prostate carcinoma cells. (A) Relative CYP2C8, 2C9 and 2J2 mRNAs normalized to HPRT1 mRNA and compared with the level of CYP2C9 mRNA in PC-3 cells (n = 5). (B) Immunoreactive bands for CYP2C8/9/19, CYP2C8, CYP2C9 and β-actin. (C) Immunoreactive band intensity of CYP2C8/9/19, 2C8 and 2C9 to the band intensity of β-actin and normalized to the intensity ratio in PC-3 cells (n = 3,4). (D) Concentrations of 11,12-EET and (E) Concentrations of 14,15-EET in prostate carcinoma cells normalized to protein content (n = 6).
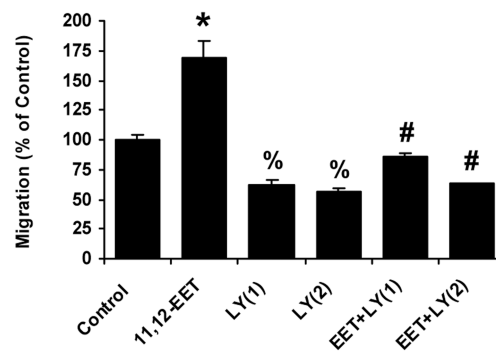
(A) Effects of 11,12-EET on cell invasion and migration
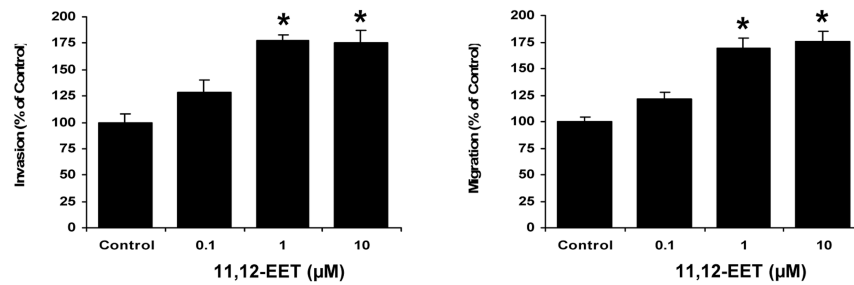
(B) Effects of a selective CYP epoxygenase inhibitor on cell invasion and migration
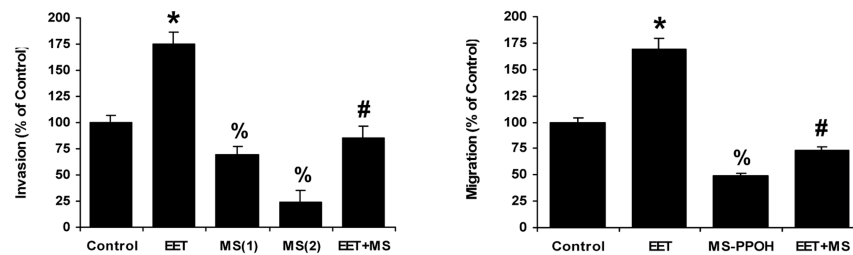
(C) Effects of a selective CYP epoxygenase inhibitor on concentrations of EETs
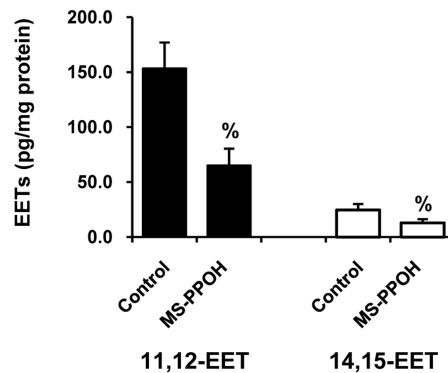
Figure 2.
Effects of EETs and a selective CYP epoxygenase inhibitor on invasion and migration. (A) Effects of 11,2-EET (0.1, 1.0 and 10.0 µmol/L) on invasion (left) and migration (right) of PC-3 cells. (B) Effects of MS-PPOH (1 = 2.0 µmol/L and 2 = 10.0 µmol/L), and a combination of 11,12-EET (1.0 µmol/L) and MS-PPOH (10.0 µmol/L) on invasion (left), migration (right, MS-PPOH = 10.0 µmol/L), and 11,12-EET-induced invasion/migration of PC-3 cells. (n = 9-12). (C) Concentrations of 11,12-EET and 14,15-EET in PC-3 cells after incubation with vehicle (control) or MS-PPOH (10.0 µmol/L) at 37°C for 30 min (n = 4). *, significantly higher than control with p < 0.01; %, significantly lower than control with p < 0.05; #, significantly lower than 11,12-EET-induced invasion or migration with p < 0.01.

## (A) Effects of an EGFR kinase inhibitor on cell migration
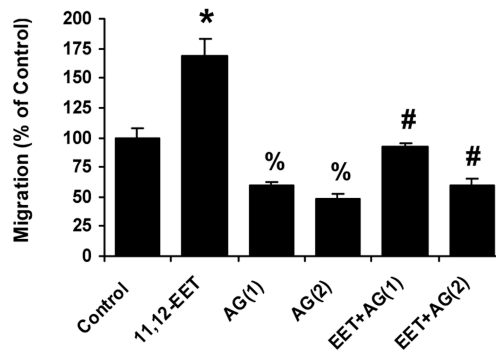
## (B) Effects of a PI3 kinase inhibitor on cell migration

Figure 3.
Effects of an EGFR kinase inhibitor and a PI3 kinase inhibitor on invasion and migration.
(A) Effects of AG-494 (AG(1) = 10.0 µmol/L, AG(2) = 20.0 µmol/L) on migration and
11,12-EET-induced migration of PC-3 cells. (B) Effects of LY294002 (LY(1) = 20.0 µmol/
L, LY(2) = 50.0 µmol/L) on migration and 11,12-EET-induced migration of PC-3 cells. (n =
9-12). *, significantly higher than control with p < 0.01; %, significantly lower than control
with p < 0.01; #, significantly lower than 11,12-EET-induced invasion or migration with p <
0.01.
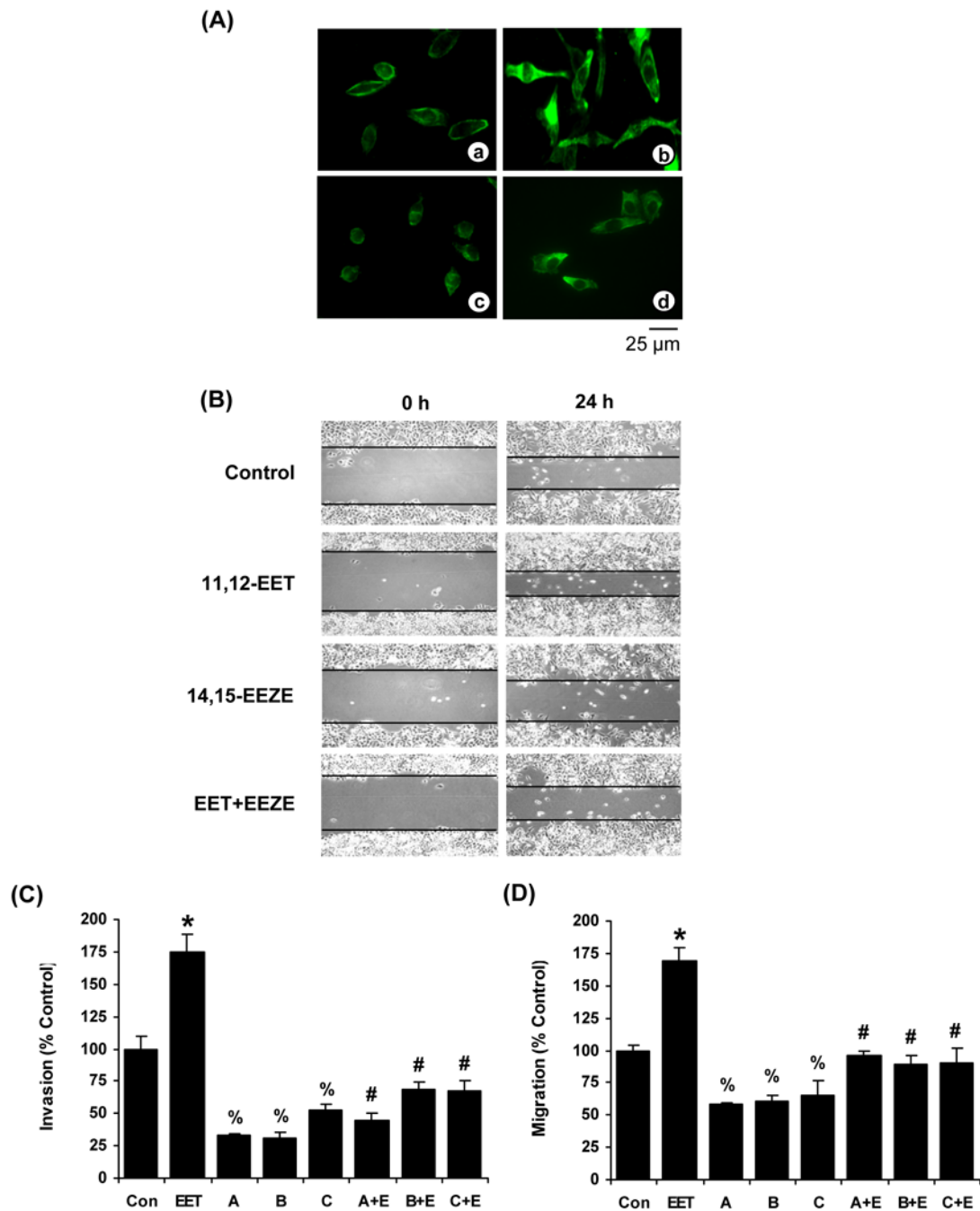
Figure 4.
Cell morphology, invasion and migration induced by EETs and EET antagonists. (A)
Fluorescence images depicting actin-myosin organization in PC-3 cells treated with (a)
vehicle, (b) 11,12-EET (1.0 µmol/L), (c) 14,15-EEZE (5.0 µmol/L), and (d) 11,12-EET and
14,15-EEZE for 90 min at 37°C. (B) Examples of effects of 11,12-EET (1.0 µmol/L), 14,15-
EEZE (5.0 µmol/L), and a combination of 11,12-EET and 14,15-EEZE on wound closures
of PC-3 cells at 37°C. (C) Effects of EET antagonists, 14,15-EEZE (**A**, 5.0 µmol/L), 14,15-
EEZE-PEG (**B**, 5.0 µmol/L), 14,15-EEZE-mSI (**C**, 5.0 µmol/L), and combinations of these
antagonists and 11,12-EET (**E**, 1.0 µmol/L) on invasion of PC-3 cells (n = 12-18). (D)

Effects of EET antagonists and combinations of these antagonists and 11,12-EET (**E**, 1.0 μmol/L) on migration of PC-3 cells (n = 9-12). *, significantly higher than control with $p < 0.01$; %, significantly lower than control with $p < 0.05$; #, significantly lower than 11,12-EET-induced invasion or migration with $p < 0.01$.
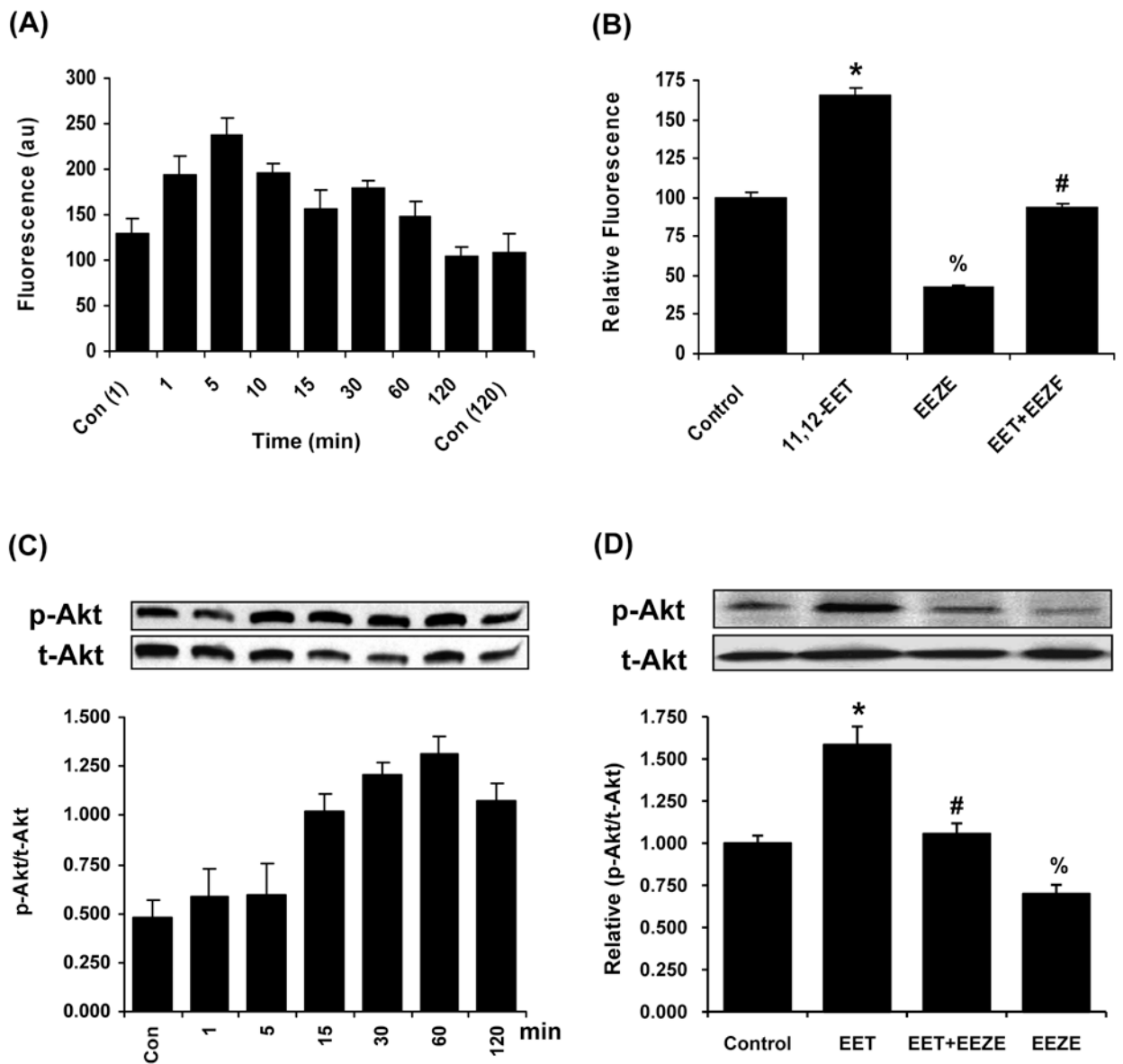
Figure 5.
Activation and inhibition of EGFR and Akt by EETs and EET antagonists. (A) Effects of 11,12-EET (1.0 µmol/L) on p-EGFR (Tyr) in PC-3 cells as determined by Bio-Plex Phospho-EGFR (Tyr) Assay Kit and normalized to t-EGFR (by Western blot) at different times and control cells at 1 min and 120 min (n = 3). (B) Effects of 11,12-EET (1.0 µmol/L), 14,15-EEZE (5.0 µmol/L), and a combination of 11,12-EET and 14,15-EEZE on p-EGFR (Tyr) at 5-min treatment and normalized to the control (n = 3). *, significantly higher than control with p < 0.01; %, significantly lower than control with p < 0.01; #, significantly lower than 11,12-EET-activated EGFR with p < 0.01. (C) Example of effects of 11,12-EET (1.0 µmol/L) on p-Akt (Ser473) in PC-3 cells at different times. Below figure is the average of the p-Akt band intensity to t-Akt at each time point (n = 4). (D) Example of effects of 11,12-EET (1.0 µmol/L), 14,15-EEZE (5.0 µmol/L), and a combination of 11,12-EET and 14,15-EEZE on p-Akt (Ser473) at 60 min treatment. Below figure is the average of the relative (p-Akt/t-Akt) in PC-3 cells treated with 11,12-EET and 14,15-EEZE as normalized to the control cells (n = 4). *, significantly higher than control with p < 0.01; %, significantly

lower than control with $p < 0.05$; [#], significantly lower than 11,12-EET-activated Akt with $p < 0.01$.
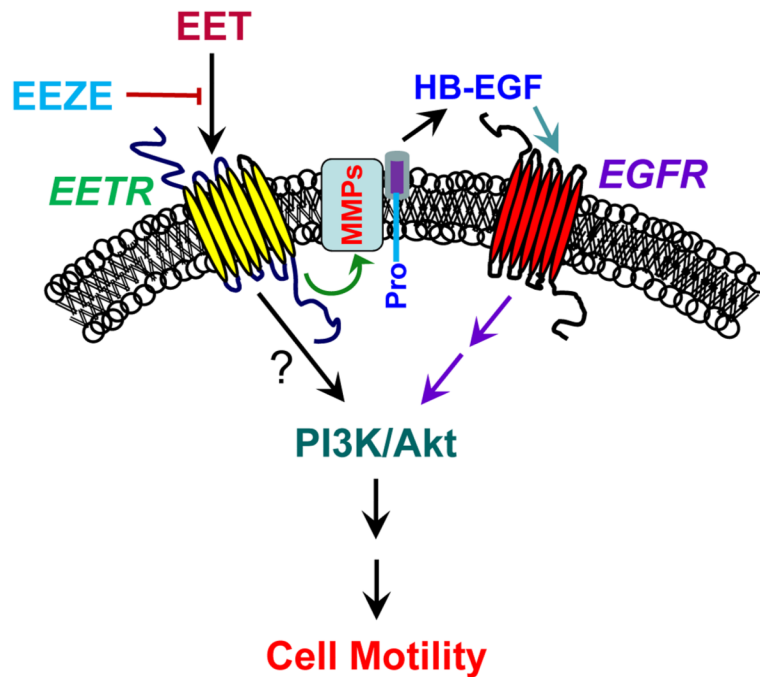
Figure 6.
A proposed diagram of signaling pathway for EET-mediated prostate carcinoma cell motility. EET = epoxyeicosatrienoic acids; EETR = putative EET receptor, EEZE; EET antagonists; EGFR = epidermal growth factor receptor, HB-EGF = Heparin-binding EGF-like growth factor; MMPs = matrix metalloproteinases. PI3K/Akt = phosphatidylinositol 3-kinase/Akt signaling pathway, Pro = Pro-HB-EGF. In this proposed signaling pathway, EETs bind to a putative EETR to activate MMPs and cleave pro-HB-EGF to HB-EGF. Then, HB-EGF activates EGFR[30,31] and initiate signaling cascade to activate PI3K/Akt pathway to increase cell motility. An unidentified mechanism of EET-activated EETR to activate PI3K/Akt signaling pathway[32] cannot be ruled out.